IEEE Access
Multidisciplinary | Rapid Review | Open Access Journal

Digital Object Identifier 10.1109/ACCESS.2020.3039198

Parameter Identification for Cells, Modules, Racks, and Battery for Utility-Scale Energy Storage Systems

OLUWASEUN M. AKEYO, VANDANA RALLABANDI*, (Senior Member, IEEE), NICHOLAS JEWELL+, (Senior Member, IEEE), ARON PATRICK+, AND DAN M. IONEL, (Fellow, IEEE)

SPARK Laboratory, ECE Department, University of Kentucky, Lexington, KY, USA
+Louisville Gas and Electric and Kentucky Utilities, Louisville, KY, USA

Corresponding author: Dan M. Ionel (e-mail: dan.ionel@ieee.org).

* Dr. Vandana Rallabandi was with the SPARK Laboratory, ECE Department, University of Kentucky, Lexington, KY and is now with GE Research, Niskayuna, NY.

ABSTRACT The equivalent circuit model for utility-scale battery energy storage systems (BESS) is beneficial for multiple applications including performance evaluation, safety assessments, and the development of accurate models for simulation studies. This paper evaluates and compares the performance of utility-scale equivalent circuit models developed at multiple sub-component levels, i.e. at the rack, module, and cell levels. This type of modeling is used to demonstrate that the equivalent circuit model for a reference cell, module, or rack of a BESS can be scaled to represent the entire battery system provided that the battery management system (BMS) is active and functional. Contrary to the rapid pulse discharge cycles employed in conventional cell parameter estimation approaches, the study proposes a new charge/discharge cycle for identifying the equivalent circuit parameters for utility-scale battery systems using equipment readily available at installation sites without the need for laboratory setups. Furthermore, a sensitivity analysis for classifying and quantifying the effect of each equivalent circuit parameter on the performance of the proposed battery system model was executed. The measurements and simulations are conducted for a 1MW/2MWh BESS testing facility located at the Louisville Gas and Electric and Kentucky Utilities (LG&E and KU) E.W. Brown generating plant. The results indicate that for the example utility-scale battery setup with an active BMS, the equivalent circuit model of either the cell, module, or rack can be scaled to represent the battery system with less than 1% average voltage error.

INDEX TERMS Battery energy storage systems, equivalent circuit, parameter estimation, racks, modules, cells, sensitivity analysis, thermal runaway, battery management system.

I. INTRODUCTION

ACCORDING to the EIA, utility-scale BESS in the U.S. account for more than 75% of the total energy storage capacity installed in 2018 [1]. The future electric grid may be able to take advantage of these predominantly Lithium-ion (Li-ion) based BESSs at the distribution, transmission and generation levels for multiple applications including voltage and frequency support, load leveling and peak power shaving, spinning reserve, and other ancillary services [2]. However, recent developments surrounding Li-ion based battery safety and thermal runaway have further emphasized the need for advanced battery monitoring systems to ensure safe operation [3], [4].

The terminal voltage of Li-ion battery energy storage varies with multiple parameters including state of charge (SOC) and mode of operation. Hence, utility-scale BESS may see variations over 200V in their dc terminal voltage during regular operation [5]. Battery systems in some cases have been represented as constant voltage sources [6]–[8], or modeled as a controlled voltage source [9]. Furthermore, recent studies have focused on small-scale battery modeling with greater emphasis on single cell operations [10]–[12]. Other researchers have worked towards developing standardized procedures for the estimation of the parameters of a single cell. [13]–[16].

Contrary to conventional approaches, in which equivalent

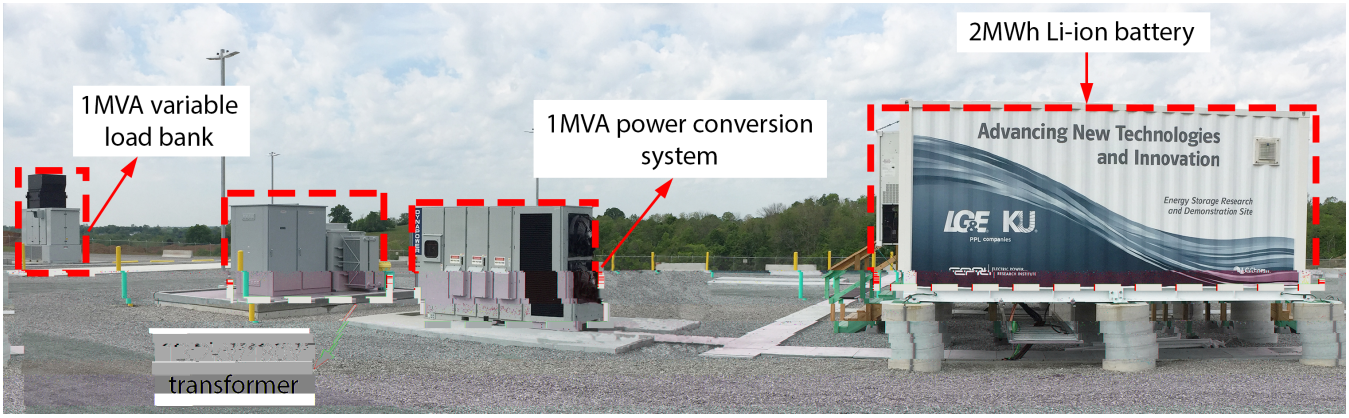

FIGURE 1. An example battery energy storage system (BESS) setup including a 1MVA bidirectional inverter, 2MWh battery system distributed in two containers(one obscured by the other), and an advanced SCADA facility, which is not shown. The 2MWh battery system incorporates 4,760 cells (20 racks or 340 modules) connected in series and parallel to meet power conditioning devices requirements.

circuit parameters for battery cells were only extracted from laboratory setups and scaled to represent the parameters of a utility-scale battery system with multiple cells and BMS [17]–[19], the proposed approach accounts for the contributions of the BMS in cell voltage balancing and acknowledges the differences in the parameter of cells from the same manufacturer.

This paper presents an approach for estimating the equivalent circuit parameters of a utility-scale battery system and its sub-components using equipment typically available at installation sites. Additionally, the work emphasizes how the difference in parameters of cells within a battery system can lead to significant variations in terminal voltages and defines a metric for comparing the voltage performance of utility-scale battery models developed using select cell, module, or rack parameters.

Furthermore, this study introduces a multi-hour operation cycle that ensures battery voltage equilibrium for each charge or discharge procedure as opposed to the conventional quick pulse discharge cycles used for battery equivalent circuit parameter estimation [20], [21]. The proposed procedure benefits from measurements of the type recommended by the new Electric Power Research Institute (EPRI) BESS test manual [22], and may also serve as a possible extension to the initiative. This work is a substantial expansion to a previous conference paper by the same group of authors [23]. Additional contributions include sensitivity analyses to establish the impact of each parameter on the system performance, and comparison of the voltage variation of the battery system to equivalent circuit models from the parameters identified from specified racks, modules, and cells.

The technical details of the 1MW/2MWh battery system employed for this analysis are presented in the second section of this paper. Section III deals with the battery operation cycles employed for the battery parameter identification and approach for validation. Section IV described the proposed test procedures adopted for the cell, modules, rack, and the battery system equivalent circuit parameter identification. The sensitivity analyses of the battery equivalent circuit components and validation of the identified parameters are presented in Sections V and VI, respectively. Finally, Section VII provides the concluding remarks and highlights the contributions of the presented study.

II. FIELD IMPLEMENTATION SETUP

This study employs a utility-scale BESS, which includes a 2MWh battery system, a 1MVA bidirectional power conversion system (PCS), a 13.2kV/480V step-up transformer, and a 1MVA programmable load bank (Fig. 1). At the time of installation, this field system was one of the largest BESS testing facilities in the US, whose capabilities have been highlighted through complex tests described in [22]. This unique setup includes advanced measurement devices capable of capturing voltage, current, and power measurements at the dc-link, inverter ac terminal, and the point of common coupling, that are synchronized with the local time and logged at one-second intervals by the SCADA system.

In order to meet the ratings of the power conditioning device, the experimental battery system includes 20 racks, which are equally distributed between two identical containers. A rack includes 17 LG Chem M48126P3B1 battery modules, each with 14 Li-ion cells and rated for 126Ah at 51.8V nominal voltage. This battery system also employs a BMS, whose function includes the supervision of cell performance and balancing the SOC across all cells. The BMS provides additional details on the battery system and sub-component state including; the measured terminal voltage of all the cells, modules, and racks; the terminal current for each rack; and the calculated SOC of individual modules, racks, and entire battery system.

The PCS is a 1MVA Dynapower bidirectional two-level converter, which may be operated at 740-1150V dc-link voltage while maintaining a constant 480V three-phase voltage on the ac side. For the purpose of carrying out multiple discharge tests with reduced grid disturbance and enable BESS operation in the isolated mode, the system is equipped with a

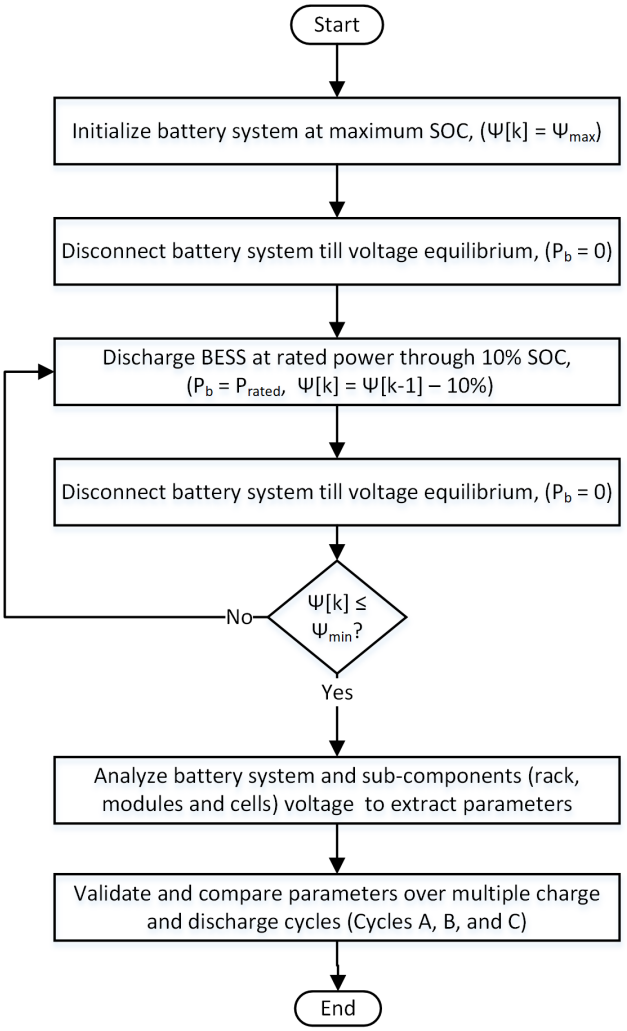

FIGURE 2. Flowchart for the experimental procedures employed in the proposed parameter extraction. The battery system is open-circuited or kept in the "float mode" in between tests in order to ensure voltage and chemical equilibrium among all cells.

1MVA, 480V three-phase Simplex programmable large size load bank, which is capable of absorbing up to 1MW resistive power and sourcing/absorbing reactive power up to 600kVAr at 5kVA load steps (Fig. 1).

III. PROPOSED TEST PROCEDURES AND MEASUREMENTS FOR THE BATTERY SYSTEM

The parameters of a battery cell vary with different factors including, temperature, state of health, state of life, depth of discharge, and SOC. Cells within a large battery system have unique characteristics and parameters even if they are identical models from the same manufacturer. Furthermore, in large multi-MW BESS, the cells are subjected to different operational conditions and load due to the presence of the BMS, which is employed for protection, monitoring, and SOC balance across all the cells. Hence, for the purpose of modeling a large battery, simply scaling the equivalent circuit parameters of a single cell may not be sufficient to represent the system accurately.

The experimental setup includes multiple advanced measuring and protection devices capable of capturing and recording high-resolution voltage, current, and SOC measurements from each cell, module, rack, and the entire BESS. This approach assumes the battery system and its components can be subjected to similar charge and discharge cycles to estimate their individual equivalent circuit parameters.

The sequence of testing begins with the initialization of the battery system at its manufacturer recommended maximum SOC, and afterward open-circuited for a long period to ensure chemical and voltage equilibrium (Fig. 2). The experimental BESS setup was subjected to multiple charge and discharge cycles and its responses including the measured battery system and sub-component terminal voltage and current, the BMS computed SOC, and the PCS real and reactive power were recorded. The battery system enclosed chamber was regulated at 23°C throughout all tests to ensure minimum temperature variation between system cycles and battery sub-components.

For this example utility-scale battery system, the recommended minimum and maximum SOC limits from the manufacturer are 5% and 95%, respectively. At the time of this research, the standard time for a utility-scale battery system to reach equilibrium had not been described. Hence, a rest period of 8h before tests and 2h after each pulse operation is proposed for the battery system based on voltage response observations. The BESS operation and voltage response were analyzed and validated over three charge/discharge cycles described as follows.

Cycle A: This cycle is used for the main parameter extraction and validation. From the system reported maximum SOC, the BESS was continuously discharged at rated power through 10% SOC and operated in the float mode for 2 hours in order to allow the battery system to approach equilibrium [22]. The float mode operation enables the battery system to approach chemical equilibrium while maintaining it at reference SOC by trickle charging at a rate equal to its self-discharge. This pulse discharge procedure was repeated until the system SOC reached the minimum. Conventional approaches require pulse discharging the battery cell at constant current. The proposed procedure is adapted to the equipment typically available at a utility-scale BESS, and therefore, the PCS is controlled for pulse discharging the battery based on a power command. In this approach, Cycles B and C are proposed for validation of the parameters identified through Cycle A.

Cycle B: This cycle is based on the exemplary performance and functionality test cycle described in [22] for characterizing the energy storage system. In this cycle, the BESS was initialized to the manufacturer recommended maximum SOC and left in the float mode till the battery system is presumed to have reached chemical and voltage equilibrium. The battery is then continuously discharged at rated power till minimum SOC, and promptly charged back to maximum SOC before being discharged once again at rated power

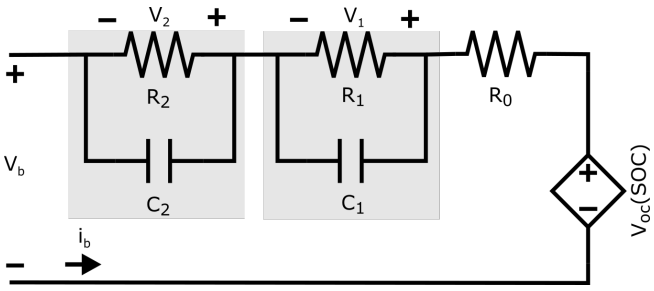

FIGURE 3. Equivalent circuit model for the battery system and its sub-components (racks, modules and cells) used for the study. Each parameter corresponds to the combination of cells connected in series and parallel.

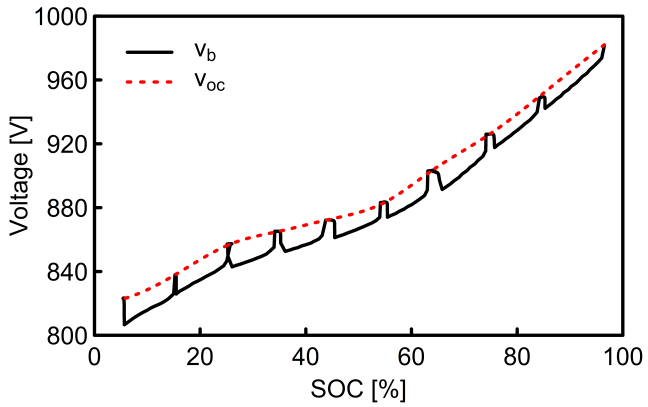

FIGURE 4. Battery system open circuit voltage. The BESS was pulse discharged (Cycle A), and the maximum dc terminal voltage (v_b) for defined SOC ranges when the output current approaches zero were used to estimate its open-circuit voltage (v_{oc}).

till 50% SOC. The BESS is then left in float mode for approximately 2 hours before the next cycle at 75% capacity of rated power. The procedure is repeated for 50% rated power and all relevant system component parameters were measured and recorded.

Cycle C: The field implemented BESS setup is co-located with multiple generation resources including solar, natural gas combustion turbines, hydropower plants, and coal-fired units with over 1GW of combined net-generation capacity. In this cycle, the BESS is operated in the autonomous frequency response mode, in which the battery charges when the frequency exceeds the reference value and discharges otherwise. Due to the reduced frequency variation near the grid-connected BESS, the response sensitivity was increased such that the battery addresses deviations greater than 0.005Hz and supports the grid at rated power for deviations above 0.05Hz based on the specified droop control.

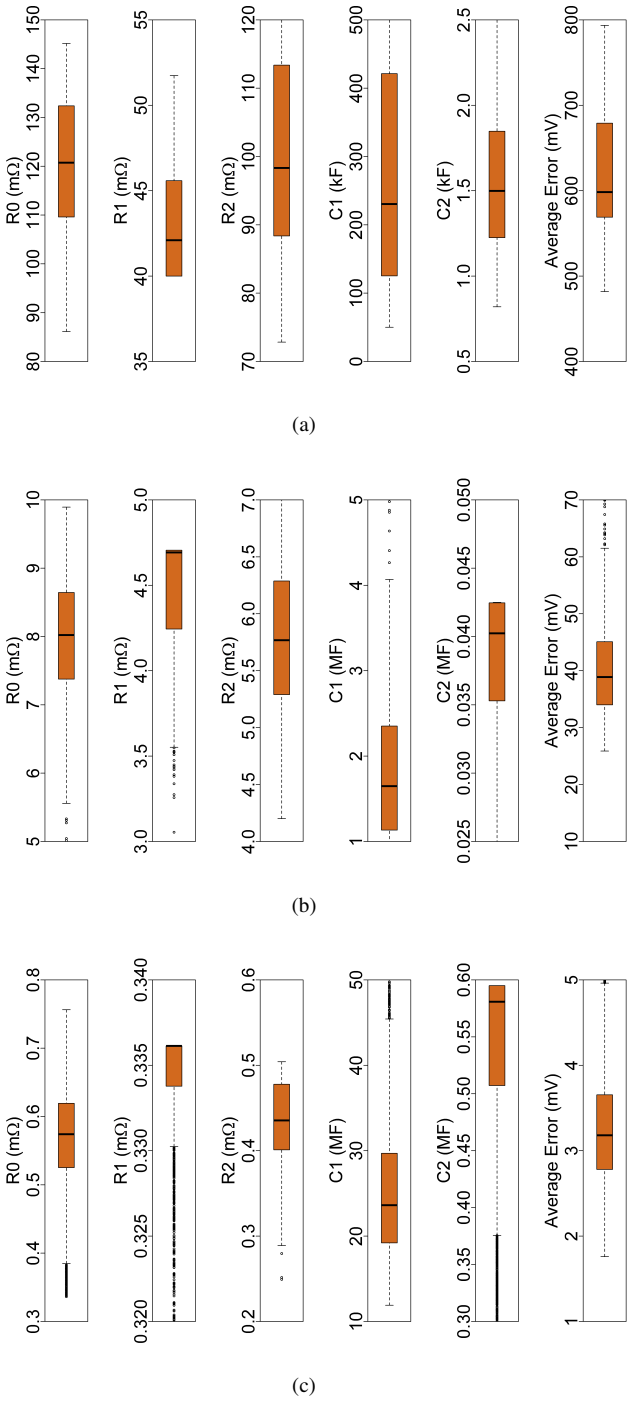

FIGURE 5. The variation of the equivalent circuit parameters for the battery systems component extracted through measurements for all (a) 20 racks, (b) 340 modules, and (c) 4,760 cells. The results illustrate typical variations within battery system sub-components from the same manufacturer.

IV. BATTERY SYSTEM, RACKS MODULES AND CELLS PARAMETER EXTRACTION

A battery cell may be represented as a controllable voltage source (v_{oc}) connected in series to a resistance (R_0) and multiple RC branches (R_1, R_2, C_1 and C_2). In this approach, it is assumed that the same type of equivalent circuit can be used to represent the battery system, rack, module, and cell, with the parameters modified accordingly (Fig. 3). The impact of parameters such as the number of charge/discharge cycles, depth of discharge, state of health, and temperature are beyond the scope of this study. Hence, the voltage response of the battery system and its sub-components are represented as

functions of SOC. It may be noted that the parameter value has been demonstrated to be minimally impacted by the SOC when the battery is operated between 5-95% [24]–[26].

The battery system terminal voltage, v_b during discharge may be described as:

$$v_b(t) = v_{oc} - i_b\,R_0 + i_b\,R_1\,e^{-\frac{\Delta t}{R_1 C_1}} + i_b\,R_2\,e^{-\frac{\Delta t}{R_2 C_2}}. \quad (1)$$

$$v_b(t) = v_{oc} - i_b\,R_0 - v_1(t) - v_2(t), \quad (2)$$

where, v_{oc}, is the battery open-circuit voltage; i_b, the battery dc output current; v_1 and v_2 , the voltages across the RC branches 1 and 2, respectively and t, the discharge duration. The voltage response of the battery system and its sub-components during BESS pulse discharge operation (Cycle A) were analyzed and used to estimate the corresponding equivalent circuit parameters. From (2), the battery terminal voltage approaches its open-circuit value as the output current tends to zero and is expressed as:

$$v_{oc}(t) = \lim_{\substack{i_b \to 0 \\ \Delta t \to \infty}} v_b(t). \quad (3)$$

In this approach, the battery and sub-components dc terminal voltages, v_b, when the current is nearly zero during Cycle A were isolated and divided into 20 SOC class intervals of the same range. Due to the influence of external parameters such as self-discharge rate and battery trickle charge, terminal voltage reduction may also be observed during open-circuit conditions. The maximum dc voltage for each bin when the output current is zero is identified as the open-circuit voltage for the reported SOC and termed as:

$$v_{oc}(\psi_i) = \max_{i_b=0}[v_b(\psi_l), v_b(\psi_u)], \qquad \psi_l \le \psi_i \le \psi_u \quad (4)$$

where, ψ_i represents the SOC corresponding to the reported class interval maximum voltage, ψ_l and ψ_u the lower and upper boundary of the select class interval, respectively. For Cycle A evaluation, only bins where the battery output current is zero were analyzed. The defined points were fit to establish the battery system open-circuit voltage relationship with SOC and a similar procedure was employed for all its racks, modules, and cells (Fig. 4).

This approach employs an artificial computation intelligence program to estimate the best values of the resistance and capacitance that can be applied to (1) for an accurate estimation of the battery terminal voltage. The fitness function is defined as the absolute value of the difference between the reported battery terminal voltage and the corresponding calculated value at each data point of Cycle A. Hence, the particle swarm optimization problem is formulated as follows:

$$\min_x F(x) = \min_x \sum_{k=1}^{M} |v_b^*(k) - v_b(k)| \quad x \in X \quad (5)$$

$$x = (R_0, R_1, R_2, C_1, C_2) \quad (6)$$

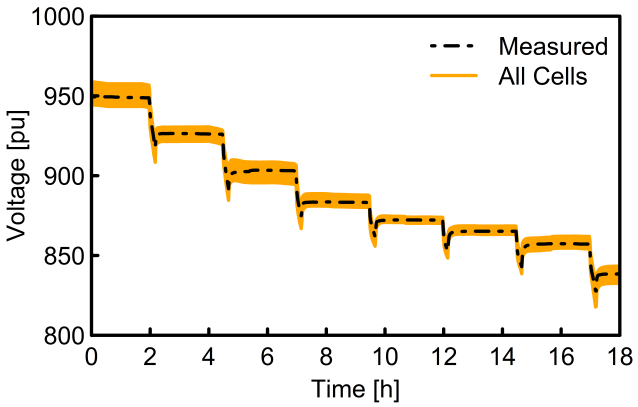

FIGURE 6. Voltage response for multiple battery system models developed as a scaled version of each individual cell from fig 5. Depending on the reference cell selected, up to 10V mismatch in the estimated battery voltage may be recorded.

where $F(x)$ is the objective function extracted from (1); k, the index of the data sample; $v_b^*(k)$, the measured battery voltage at the kth data sample; $v_b(k)$, the calculated battery voltage at the kth data sample; M, the number of data samples; x, is the vector with all the battery parameters; and X, is the space of solutions.

A satisfactory average voltage error less than one-percent was reported for Cycle A when the battery models developed using a combination of the established open-circuit voltage and SOC relationship with parameters retrieved from the optimization process for the battery system all its sub-components were compared to the reported values. Even though all the cells that make up individual modules, racks, and the entire battery system are from the same manufacturer, a significant disparity can be observed in their estimated parameters (Fig. 5).

V. PARAMETERS SENSITIVITY ANALYSIS

In order to identify the most influential parameters affecting the accuracy of the battery equivalent circuit model presented in Fig. 3, a sensitivity analysis was conducted. A regression model was employed to relate the identified battery system parameters. In this approach, a 2^{nd} order polynomial function with a goodness-of-fit, R^2, above 90% was employed and expressed as follows:

$$Y = \beta_0 + \sum_{i=1}^{d_\nu} \beta_i X_{Ci} + \sum_{i=1}^{d_\nu} \beta_{ii} X_{Ci}^2 + \sum_{i=1}^{d_\nu} \sum_{j=i+1}^{d_\nu} \beta_{ij} X_{Ci} X_{Cj}\,, \quad (7)$$

$$X_{Ci} = \frac{x_i - (x_{i,max} + x_{i,min})/2}{(x_{i,max} - x_{i,min})/2}\;;\; i = 1, 2, ..., d_\nu, \quad (8)$$

where Y is the response parameter; β, the regression coefficient; d_ν, the number of factors, x_i, the i^{th} input factor; and X_{Ci}, the normalized (coded) value of the i^{th} factor. Factors

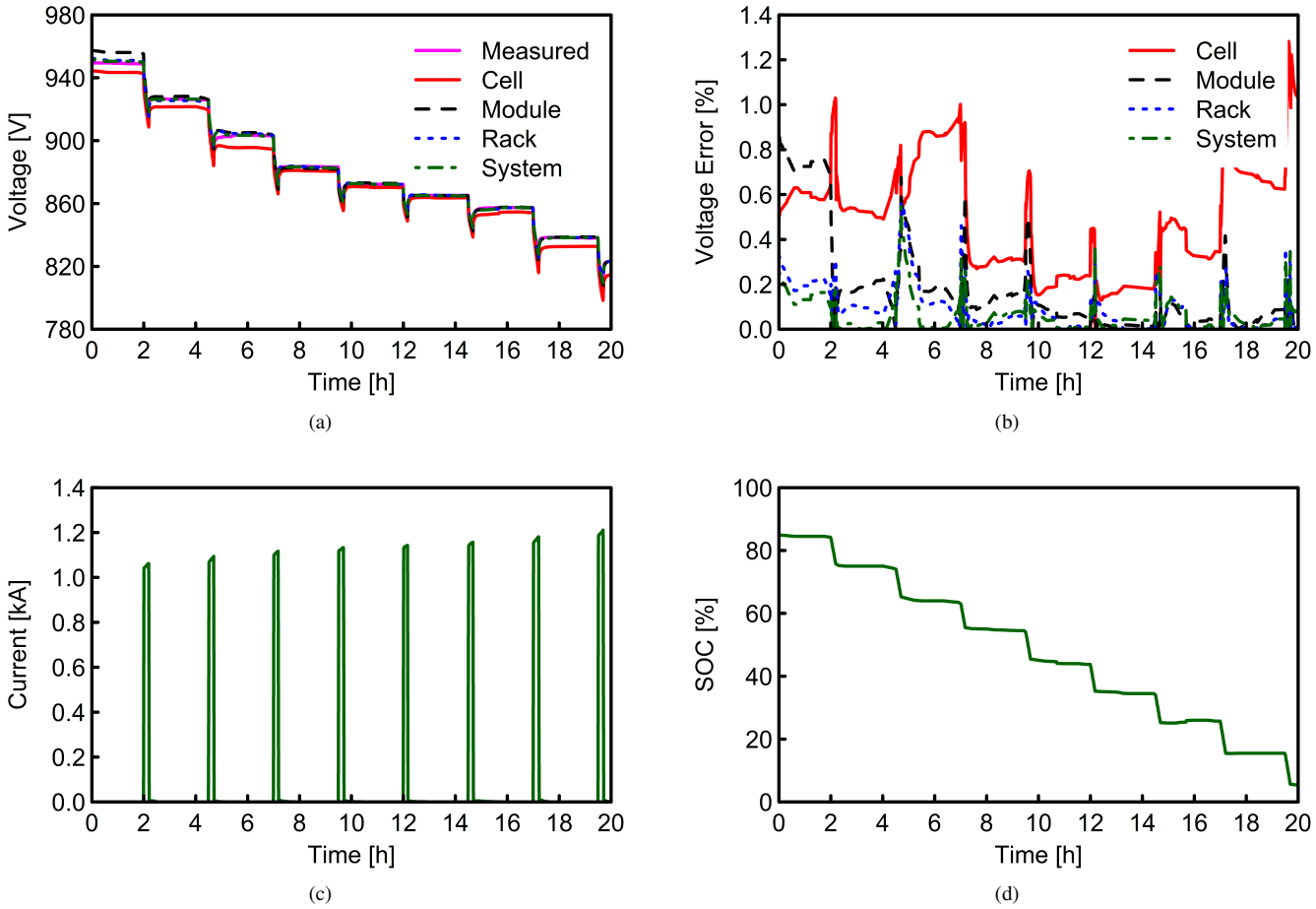

FIGURE 7. The BESS during rated power pulse discharge from maximum to minimum SOC showing: (a) The experimental and simulated battery system terminal voltage variation for the system and sub-components, (b) the percentage voltage error, (c) the discharge current, (d) and the SOC variation. The battery discharge current increases to maintain constant pulse discharge power as voltage decreases with SOC.

may be normalized as shown in (7). $X_{Ci} = 0$ represents the specified values of the factors with the reference response, and β_0 is a representation of response parameter in this reference situation. β_{ii} and β_{ij} illustrate second order effects and interaction between the factors.

In this approach, the voltage responses of 15,625 equivalent circuit models for the battery system with each parameter varying between $\pm 10\%$ of the extracted value were analyzed over Cycle A. The results of the sensitivity analysis with regards to the average and peak voltage error of the battery system are presented in Table 1. The main takeaways from the study are as follows:

1) The open-circuit voltage of the battery is the main parameter that influences the voltage response of the system

2) Depending on the cycle analyzed the RC branch parameters are the least significant

3) The battery series resistance, R_0 has an observable effect on the maximum voltage error recorded.

TABLE 1. Sensitivity Analysis Regression Co-coefficients

Parameters	Average Error [pu] $\times 10^{-3}$	Max Error [pu] $\times 10^{-2}$
R_0	-0.09	1.10
R_1	0.07	-0.02
R_2	-0.04	-0.08
C_1	0.02	0.02
C_2	0.01	-0.36
v_{oc}	3.85	4.46

VI. BATTERY SYSTEM PARAMETER VALIDATION AND COMPARISON

The sequence of validation was initiated with a comparison of the multiple battery system models developed as a scaled version of all 4,760 cells in the considered 1MW/2MWh setup. For validation purposes, this approach assumes that battery sub-components contribute equal currents and voltages to represent the entire battery system. Hence, each sub-component current is defined as a fraction of the total battery system current and the total amount of component strings in parallel, while the corresponding sub-component voltage

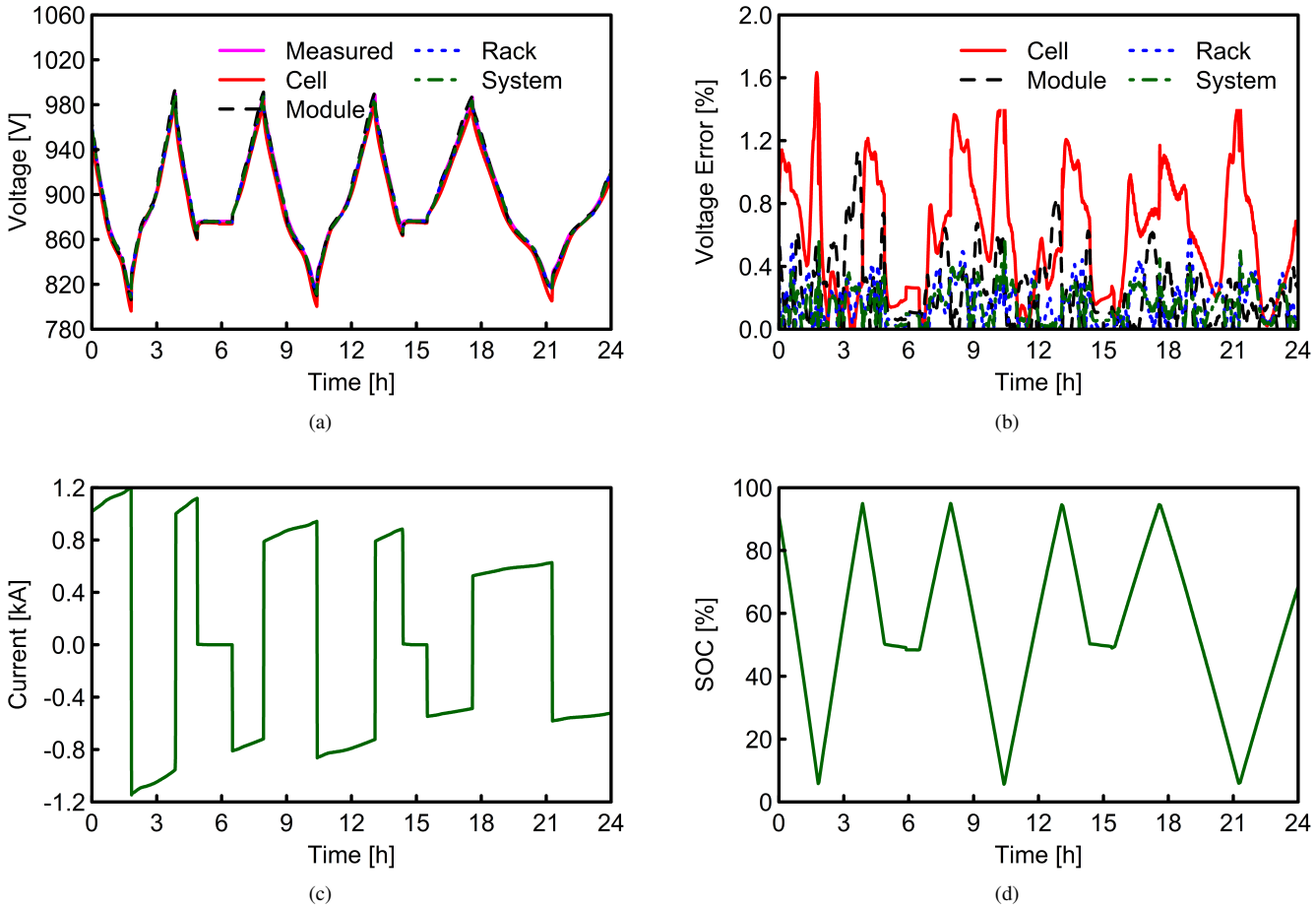

FIGURE 8. The BESS during dynamic charge and discharge between multiple SOC levels at 100%, 75% and 50% power rating ($CycleB$) showing: (a) The experimental and simulated battery system terminal voltage variation, (b) the percentage voltage error, (c) the discharge current, (d) and the SOC variation. The average error for the system and selected sub-components were considered to be within acceptable limits and the maximum percentage error was reported for the representative cell.

represents a fraction of the total number of components in series per string(Table 2). The analysis showed that for the example setup considered, the average voltage error of a battery system modeled can vary up to 10V depending on the reference cell selected (Fig. 6). Also, the performance evaluation reported higher disparities in the simulated voltages at SOC greater than 50%.

The accuracy of a battery equivalent circuit for utility-scale systems does not only depend on the reference member of the sub-component but also the sub-level analyzed. In order to demonstrate this, the battery terminal voltage was derived using three scaling approaches: scaling the voltage from a) the cell; b) the module, and c) the rack levels, and compared with the terminal voltage predicted by the proposed method based on tests conducted at the battery level.

The terminal voltage predicted by the battery models developed using scaled parameters of the select combination of cell, module, and rack sub-components with the highest average error was evaluated through Cycle A (Fig. 7). It can be observed that the simulated voltage responses of these models developed using sub-component parameters were within acceptable limits, which may be attributed to the presence of the BMS ensuring that all measured cell voltages are typically within 3mV variation. In this approach, the percentage voltage error was calculated as:

$$\% \text{ Error} = \frac{|V_{exp} - V_{sim}|}{V_{exp}} \times 100 \tag{9}$$

where V_{exp} and V_{sim} represent the measured and simulated battery system voltage responses, respectively. It can be observed that the recorded voltage variation of the battery system model developed from scaling the cell parameters has lower accuracy compared to the system alternative, which had less than 0.1% average error for the cycle (Table 3).

The performance of the developed battery models is validated for steady-state operation, as well as grid frequency regulation. For the steady-state case, the simulated voltage variations of the battery sub-component models were compared with the measured BESS dc-link terminal voltage when subjected to Cycle B power variation (Fig. 8). In this operation cycle, the influence of the RC branch parameters is

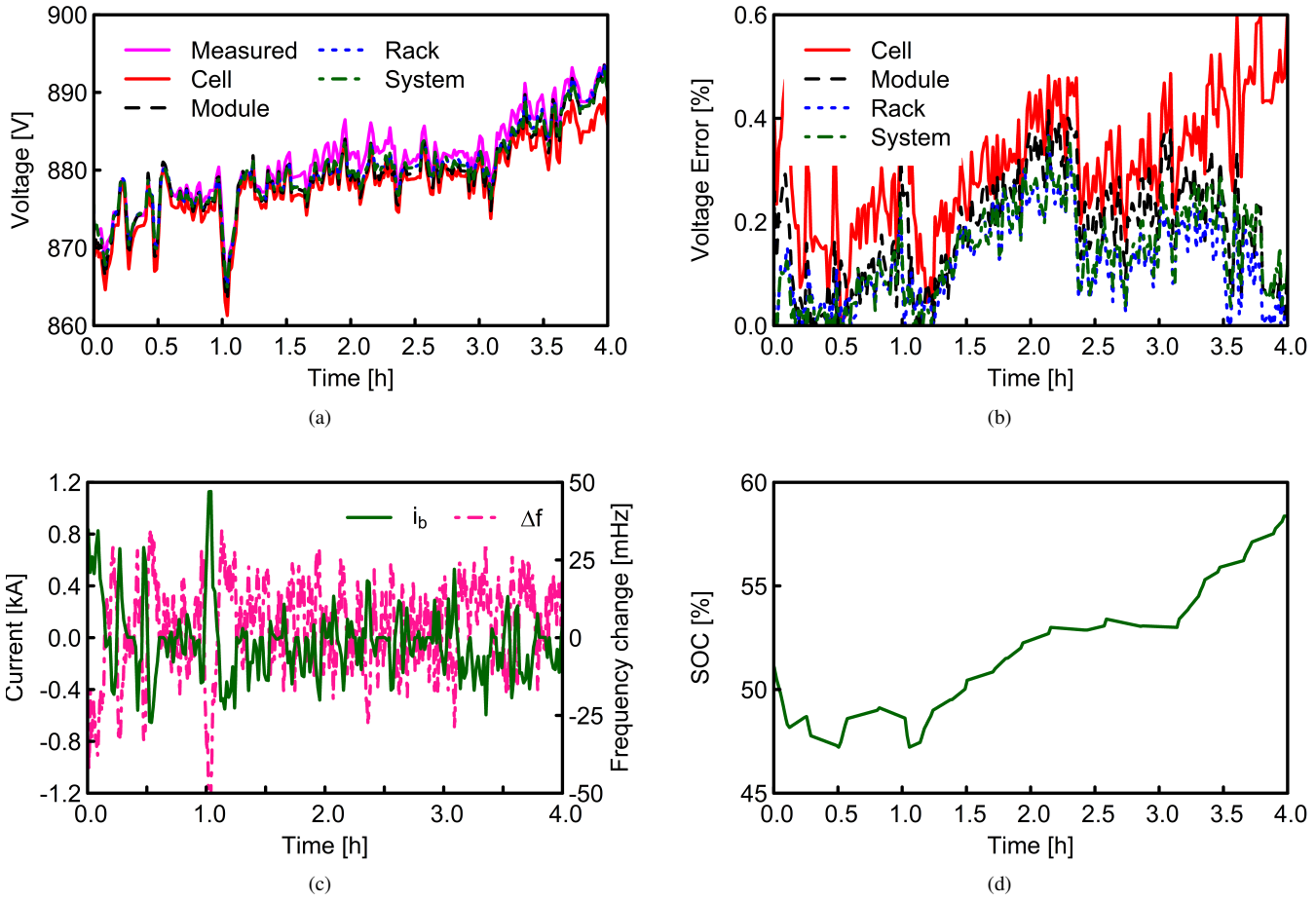

FIGURE 9. The BESS during automated grid frequency response, showing: (a) The experimental and simulated battery system terminal voltage variation for the battery system and sub-components, (b) the percentage voltage error, (c) the discharge current(i_b) and grid frequency deviation (Δf), (d) and the SOC variation.The BESS sensitivity was modified such that the system responds to frequency deviations about 5mHz.

minimal, and the recorded voltage error is primarily due to the open-circuit voltage and resistances. For this validation cycle, the equivalent circuit model developed as a function of the system parameters has the minimum mean voltage error.

Battery energy storage systems may be employed for grid frequency regulation, during which active power is provided in response to changes in frequency. The variations in terminal voltage predictions for the developed equivalent circuit models were further evaluated through the frequency response operation described in Cycle C. The fast charge and discharge operations through this cycle resulted in minimal SOC variation and increased voltage error for the system and rack models, which can be observed at SOC ranges between 53-54% (Fig. 9). It is however important to recognize that the average voltage error for the system equivalent model and sub-components are all less than 0.4% and within an acceptable range.

VII. CONCLUSION

This paper reports on the variation in the equivalent circuit parameters for the racks, modules, and cells for a utility-scale battery system and presents an approach for identifying battery level parameters using equipment typically available at installation sites. A multi-hour discharge cycle for the BESS that can identify its equivalent circuit parameters while ensuring that the battery system terminal voltage stabilizes after transient discharge operations is proposed. A comparison of the performance of the equivalent circuit models derived from this approach with those obtained scaling up the parameters for battery sub-components (i.e. cells, modules, and racks) is performed, and it is found that the scaling approach can be used to represent the entire system provided that the BMS is operational. The BESS operator can adopt these models to monitor the operation of the BMS in addition

TABLE 2. Sub-components configuration for Field Implemented 1MW/2MWh Battery System

Sub-components	Springs in parallel	String length
Cells	20	238
Modules	20	17
Racks	20	1

TABLE 3. The battery system percentage voltage errors using equivalent circuit parameters at different sub-component levels.

		Mean [%]	Max [%]
Cycle A	System	0.06	0.55
	Rack	0.09	0.58
	Module	0.18	0.87
	Cells	0.49	1.28
Cycle B	System	0.16	0.98
	Rack	0.17	1.11
	Module	0.25	1.53
	Cells	0.60	1.71
Cycle C	System	0.14	0.51
	Rack	0.12	0.52
	Module	0.18	0.45
	Cells	0.31	0.61

to other safety and simulation applications.

In order to validate the performances of the scaled equivalent circuit models and the effectiveness of the proposed approach, the simulated voltage responses of the battery system models were compared with experimental data retrieved from a 1MW/2MWh BESS, and satisfactory accuracy was observed. This work also demonstrates that the accuracy of the battery system models increases with the number of cells considered. For the example field implementation considered, average and peak voltage errors as low as 0.06% and 1.71% , respectively, were calculated with the model developed from scaling up the parameters of a single cell. This indicates that while modeling a multi-MW battery at the sub-component level may be sufficient for all practical purposes, the accuracy of models can be improved when the parameters at the battery level are determined

ACKNOWLEDGMENT

The support of LG&E and KU, and of University of Kentucky, the L. Stanley Pigman endowment is gratefully acknowledged.

REFERENCES

[1] *Battery Storage in the United States: An Update on Market Trends*. U.S. Energy Information Administration, July 2020.

[2] F. Blaabjerg and D. M. Ionel, *Renewable energy devices and systems with simulations in MATLAB® and ANSYS®*. CRC Press, 2017.

[3] C. Zhao, J. Sun, and Q. Wang, "Thermal runaway hazards investigation on 18650 lithium-ion battery using extended volume accelerating rate calorimeter," *Journal of Energy Storage*, vol. 28, p. 101232, 2020. [Online]. Available: http://www.sciencedirect.com/science/article/pii/S2352152X19311077

[4] X. Feng, M. Ouyang, X. Liu, L. Lu, Y. Xia, and X. He, "Thermal runaway mechanism of lithium ion battery for electric vehicles: A review," *Energy Storage Materials*, vol. 10, pp. 246–267, 2018.

[5] O. Akeyo, V. Rallabandi, N. Jewell, and D. M. Ionel, "Modeling and simulation of a utility-scale battery energy storage system," in *2019 IEEE Power Energy Society General Meeting (PESGM)*, 2019, pp. 1–5.

[6] H. V. Nguyen, D. To, and D. Lee, "Onboard battery chargers for plug-in electric vehicles with dual functional circuit for low-voltage battery charging and active power decoupling," *IEEE Access*, vol. 6, pp. 70 212–70 222, 2018.

[7] R. Kushwaha and B. Singh, "Power factor improvement in modified bridgeless landsman converter fed ev battery charger," *IEEE Transactions on Vehicular Technology*, vol. 68, no. 4, pp. 3325–3336, 2019.

[8] M. Y. Metwly, M. S. Abdel-Majeed, A. S. Abdel-Khalik, R. A. Hamdy, M. S. Hamad, and S. Ahmed, "A review of integrated on-board ev battery chargers: Advanced topologies, recent developments and optimal selection of FSCW slot/pole combination," *IEEE Access*, vol. 8, pp. 85 216–85 242, 2020.

[9] M. Restrepo, J. Morris, M. Kazerani, and C. A. Cañizares, "Modeling and testing of a bidirectional smart charger for distribution system ev integration," *IEEE Transactions on Smart Grid*, vol. 9, no. 1, pp. 152–162, 2018.

[10] D. Dvorak, T. Bäuml, A. Holzinger, and H. Popp, "A comprehensive algorithm for estimating lithium-ion battery parameters from measurements," *IEEE Transactions on Sustainable Energy*, vol. 9, no. 2, pp. 771–779, April 2018.

[11] C. R. Lashway and O. A. Mohammed, "Adaptive battery management and parameter estimation through physics-based modeling and experimental verification," *IEEE Transactions on Transportation Electrification*, vol. 2, no. 4, pp. 454–464, Dec 2016.

[12] H. M. Usman, S. Mukhopadhyay, and H. Rehman, "Universal adaptive stabilizer based optimization for li-ion battery model parameters estimation: An experimental study," *IEEE Access*, vol. 6, pp. 49 546–49 562, 2018.

[13] S. A. Hamidi, D. M. Ionel, and A. Nasiri, "Batteries and ultracapacitors for electric power systems with renewable energy sources," *Renewable Energy Devices and Systems with Simulations in MATLAB® and ANSYS®*, 2017.

[14] A. Biswas, R. Gu, P. Kollmeyer, R. Ahmed, and A. Emadi, "Simultaneous state and parameter estimation of li-ion battery with one state hysteresis model using augmented unscented kalman filter," in *2018 IEEE Transportation Electrification Conference and Expo (ITEC)*, June 2018, pp. 1065–1070.

[15] D. C. Cambron and A. M. Cramer, "A lithium-ion battery current estimation technique using an unknown input observer," *IEEE Transactions on Vehicular Technology*, vol. 66, no. 8, pp. 6707–6714, Aug 2017.

[16] A. M. Bizeray, J. Kim, S. R. Duncan, and D. A. Howey, "Identifiability and parameter estimation of the single particle lithium-ion battery model," *IEEE Transactions on Control Systems Technology*, pp. 1–16, 2018.

[17] R. Gu, P. Malysz, H. Yang, and A. Emadi, "On the suitability of electrochemical-based modeling for lithium-ion batteries," *IEEE Transactions on Transportation Electrification*, vol. 2, no. 4, pp. 417–431, 2016.

[18] F. Feng, X. Hu, K. Liu, Y. Che, X. Lin, G. Jin, and B. Liu, "A practical and comprehensive evaluation method for series-connected battery pack models," *IEEE Transactions on Transportation Electrification*, vol. 6, no. 2, pp. 391–416, 2020.

[19] J. Lee, J. Ahn, and B. K. Lee, "A novel li-ion battery pack modeling considerging single cell information and capacity variation," in *2017 IEEE Energy Conversion Congress and Exposition (ECCE)*, 2017, pp. 5242–5247.

[20] J. Meng, D. Stroe, M. Ricco, G. Luo, and R. Teodorescu, "A simplified model-based state-of-charge estimation approach for lithium-ion battery with dynamic linear model," *IEEE Transactions on Industrial Electronics*, vol. 66, no. 10, pp. 7717–7727, 2019.

[21] H. Chun, M. Kim, J. Kim, K. Kim, J. Yu, T. Kim, and S. Han, "Adaptive exploration harmony search for effective parameter estimation in an electrochemical lithium-ion battery model," *IEEE Access*, vol. 7, pp. 131 501–131 511, 2019.

[22] *Energy Storage Integration Council (ESIC) Energy Storage Test Manual*. EPRI, Palo Alto, CA: 2017. 3002011739.

[23] O. M. Akeyo, V. Rallabandi, N. Jewell, and D. M. Ionel, "Measurement and estimation of the equivalent circuit parameters for multi-mw battery systems," in *2019 IEEE Energy Conversion Congress and Exposition (ECCE)*. IEEE, pp. 2499–2504.

[24] Z. Yu, L. Xiao, H. Li, X. Zhu, and R. Huai, "Model parameter identification for lithium batteries using the coevolutionary particle swarm optimization method," *IEEE Transactions on Industrial Electronics*, vol. 64, no. 7, pp. 5690–5700, 2017.

[25] M. Partovibakhsh and G. Liu, "An adaptive unscented kalman filtering approach for online estimation of model parameters and state-of-charge of lithium-ion batteries for autonomous mobile robots," *IEEE Transactions on Control Systems Technology*, vol. 23, no. 1, pp. 357–363, 2015.

[26] X. Liu, W. Li, and A. Zhou, "PNGV equivalent circuit model and soc estimation algorithm for lithium battery pack adopted in AGV vehicle," *IEEE Access*, vol. 6, pp. 23 639–23 647, 2018.

OLUWASEUN M. AKEYO (S'16) received the M.S. degree in electrical engineering from University of Kentucky, Lexington, KY and the B. Eng degree in electrical and electronics engineering from Abubakar Tafawa Balewa University (ATBU), Bauchi, Nigeria in 2017 and 2014, respectively. He is currently a Ph.D. candidate in electrical engineering at University of Kentucky, where he also serves as a research assistant in the SPARK Laboratory. He won the Best Presentation award at the 2018 FEEDER Summer Program and the Best Poster Paper award at the 2016 IEEE International Conference on Renewable Energy Research and Applications, ICRERA. His research focuses on power systems, power electronics, battery energy storage, and renewable energy sources.

VANDANA RALLABANDI (M'17–SM'19) is a Lead Engineer at GE Research in Niskayuna, NY, USA. Previously, she was a Postdoctoral Researcher with the SPARK Lab, University of Kentucky, Lexington, KY, USA, and a Research Engineer with the GE Research Center, Bangalore, India. Her research interests include electric machines, power electronics drives, renewable energy devices and systems, energy storage, and power systems. She received the masters and Ph.D. degrees from the Indian Institute of Technology Bombay, Mumbai, India.

NICHOLAS JEWELL (S'07–M'15–SM'18) received the Doctor of Philosophy degree in electrical engineering from the University of Louisville, Louisville, KY, USA, in 2014. He is a Senior Electrical Engineer with the Electrical Engineering and Planning Department, Louisville Gas and Electric and Kentucky Utilities (LG&E and KU). At LG&E and KU, he serves as the company subject matter expert in areas such as distribution planning, power systems analysis, and distributed energy resources (DER). Dr. Jewell's primary focus is on implementing advanced DER strategies and defining and executing a multi-year strategic roadmap pertaining to distribution hosting capacity, distribution system interconnection requirements, customer usage behavior, and system analysis regarding DER impacts to protection systems. He has been an author or co-author for a number of industry publications, has received several Tech Transfer Awards from the Electric Power Research Institute, and has one patent disclosure. Additionally, he was named a Top Innovator by Public Utilities Fortnightly in 2018. Dr. Jewell is a Registered Project Management Professional.

ARON PATRICK manages Technology Research and Analysis for LG&E and KU. Before joining LG&E and KU, Patrick held leadership roles at the Kentucky Energy and Environment Cabinet, including assistant director and program manager for renewable energy. In those roles, he worked with policy makers, industry, national research laboratories, and universities on projects involving energy policy and future generation technologies. Prior to that, Aron was an intelligence analyst for the federal government, using statistical analysis and modeling to address national security problems. Aron is a Lexington native, with bachelor and master degrees from the University of Kentucky in international commerce, statistics, and political science.

DAN M. IONEL (M'91–SM'01–F'13) is Professor of Electrical Engineering and the L. Stanley Pigman Chair in Power at the University of Kentucky, Lexington, KY, where he is also the Director of the Power and Energy Institute of Kentucky (PEIK) and of the SPARK Laboratory. He previously worked in industry, most recently as Chief Engineer for Regal Beloit Corp., Grafton, WI, USA, and, before that, as the Chief Scientist for Vestas Wind Turbines. Concurrently, he was also a Visiting and Research Professor with the University of Wisconsin and Marquette University in Milwaukee, WI. Dr. Ionel contributed to technology developments with long lasting industrial impact, holds more than 35 patents, published more than 200 hundred papers, and co-authored 3 books. His research has been supported directly by industry, and by NSF, NIST, DOE, and NASA.

He received the M.Eng. and Ph.D. degrees in electrical engineering from the Polytechnic University of Bucharest, Bucharest, Romania. His doctoral program included a Leverhulme Visiting Fellowship with the University of Bath, Bath, U.K., and later he was a Postdoctoral Researcher with the SPEED Laboratory, University of Glasgow, Glasgow, U.K.

Dr. Ionel is an IEEE Fellow and a recipient IEEE Power and Energy Society Veinott Award. He was the Inaugural Chair of the IEEE Industry Applications Society Renewable and Sustainable Energy Conversion Systems Committee, an Editor for the IEEE Transactions on Sustainable Energy, the Chair of the IEEE PES MSC and of the IEEE WG 1812, the Technical Program Chair of 2015 IEEE ECCCE and the General Chair of the 2017 IEEE IEMDC. He is the Editor-in-Chief of the Electric Power Components and Systems Journal, and the Chair of the Steering Committee for the IEEE IEMDC Conferences.